# Sustainable Wastewater Treatment: Raw and Activated Cow Dung for the Sorption of Methylene Blue Dye

Abimbola Aina Ogundiran,[a,]* Olusegun Olafimihan Ogundiran,[b] Badeji Abosede Adejoke,[a] Ali El Gamal,[c] and Talha Bin Emran [d,e] and Mohamed Hefnawy[f]

Water pollution caused by synthetic dyes, like methylene blue, is a threat to the existence of biogenic components of the environment. This study explores the use of raw cow dung (RCD) and treated (acid treatment) cow dung (TCD) as effective sorbents to remove methylene blue (MB) from wastewater. The optimal conditions for MB removal of 58.3% (RCD) and 86.6% (TCD) were determined as 300 mg/L initial dye concentration, 120 min for RCD, and 100 min for TCD contact time, 50 °C temperature, and pH 5.0. Maximum adsorption capacity of 47.8 mg/g and 64.26 mg/g were determined for RCD and TCD, respectively. Thermodynamic parameter of enthalpy change ($\Delta H°$ = 9.32 kJ/mol for RCD and 6.40 kJ/mol for TCD) indicated an endothermic process. Fourier transform infrared spectroscopy (FT-IR) identified functional groups, such as OH, -$NH_2$, C=O, and C-O, as being responsible for the uptake of the dye molecules. The study confirms that activated cow dung is a sustainable, cost-effective alternative to conventional adsorbents like activated carbon for dye removal.

*DOI: 10.15376/biores.20.3.6815-6836*

*Keywords: Adsorption; Cow dung; Kinetics; Methylene blue; Thermodynamics*

*Contact information: a: Department of Chemical Sciences, Tai Solarin University of Education, Ijagun, Ogun State, Nigeria; b: Department of Chemistry, Sikiru Adetona College of Education, Science and Technology, Ije-Omu, Ogun State; c: Department of Pharmaceutical Chemistry, College of Pharmacy, King Saud University, Riyadh 11451, Saudi Arabia.; d: Department of Pathology and Laboratory Medicine, Warren Alpert Medical School, Brown University, Providence, RI 02912, USA; e: Department of Pharmacy, Faculty of Health and Life Science, Daffodil International University, Dhaka 1207, Bangladesh; f: Department of Pharmacognosy, College of Pharmacy, King Saud University, Riyadh 11451, Saudi Arabia; * Corresponding author: abimbolaogundiran701@gmail.com*

## INTRODUCTION

The disposal of effluents containing dye into aquatic systems presents significant issues as the presence of contaminants, like dye, in the environment has a negative impact on ecosystem and human health. Industries, like textiles, paper, leather, plastics, and cosmetics, are significant contributors to water pollution and release high amounts of synthetic dyes into the water system (Métivier-Pignon *et al*. 2003; Rafatullah *et al*. 2010; Iwuozor *et al*. 2022). Around 700,000 tons of various commercial dyes are manufactured each year, and a large portion of it accumulates in the wastewater (Dawood *et al*. 2017; Ahmad *et al*. 2020). In addition to creating aesthetic problems, these dyes release pollutants harmful to human health and aquatic organisms. These dyes pose not just aesthetic issues, but also hazardous materials that threaten aquatic life and human health.

Methylene blue is a common synthetic dye often used in various industries, such as papermaking, textiles, and healthcare (Ofudje *et al.* 2024). It is a cationic dye, which includes linked aromatic rings and a dimethyl amino group that makes it structurally stable (Shahryari *et al.* 2010). Although MB has many uses, it is also a recognized carcinogen that, when ingested or inhaled, can result in major health issues like skin irritation, respiratory issues, and gastrointestinal distress (Dawood *et al.* 2017). Additionally, MB disrupts photosynthesis in aquatic environments by obstructing sunlight penetration and preventing water body reoxygenation (Oveisi *et al.* 2018).

Therefore, MB removal from wastewater is crucial for environmental and public health protection. Numerous methods, including coagulation-flocculation, advanced oxidation, and membrane filtration processes, have been studied for dye removal; however, their use is restricted because of their high operating costs, the creation of toxic sludge, and their inability to remove all of the dye (Bielska and Szymanowski 2006; Geed *et al*. 2019; Tsai *et al*. 2019; Mashkoor and Nasar 2020; Santoso *et al*. 2020, Sonwani *et al*. 2020). Furthermore, the presence of stable aromatic structures that hinder biodegradation and are resistant to light and oxidative chemicals makes it more difficult to remove many synthetic dyes from wastewater using traditional water treatment methods (Shokoohi *et al*. 2010; Faraji *et al.* 2015; Ahmad *et al.* 2020). Given these problems, it is essential to find cost-effective, environmentally responsible, and efficient wastewater treatment alternatives to traditional methods.

Particularly for industries dealing with dye and heavy metal removal, adsorption is a preferred option due to its effectiveness, affordability, and environmental friendliness. It can remove a variety of contaminants with little to no secondary pollution (Ahmad *et al*. 2015; Crini and Lichtfouse 2019). Commercial adsorbents, such as zeolites, activated carbon, or modified biochar, can be expensive to develop and, as a result, frequently restrict the operation of adsorption, despite their benefits (Ahmad *et al*. 2015; Crini and Lichtfouse, 2019). To overcome this challenge, researchers concentrate on using inexpensive biosorbents derived from microbes, animals, and agricultural wastes as a practical method of eliminating colors from aqueous solutions.

Cow dung is a common and easily accessible biomass in rural regions that has attracted attention due to its potential for biosorption. Dung from cows is a desirable biosorbent for wastewater treatment because of its organic matter, cellulose, lignin, proteins, and microbial populations, which offer active sites for pollutant binding (El-Rayyes *et al*. 2025). Cow dung has been shown in numerous studies to be an excellent way to remove a variety of contaminants, like organic compounds and heavy metals (Qian *et al*. 2008, 2009; El-Rayyes *et al*. 2025). Because both untreated and treated cow dung have demonstrated potential as biosorbents, it is crucial to assess their capacity for adsorption and how they interact with various pollutants (Zhu *et al*. 2018; Iwuozor *et al*. 2022). Several functional groups, including carboxyl, amine, hydroxyl, and carbonyl components, aid in the uptake of contaminants from wastewater (Zhu *et al.* 2020; Chen *et al*. 2022). Cow dung is increasing due to Nigeria's increased cow output, and it would be ideal to turn it into a useful product, such as an adsorbent for the treatment of wastewater.

The structural integrity and aqueous stability of bio-based adsorbents, such as cow dung-derived materials, are critical considerations for their practical application in water treatment. While cow dung has been reported as a low-cost and effective adsorbent due to its fibrous structure and high organic content, concerns remain regarding its potential dissolution, microbial degradation, or release of particulate matter when exposed to water for extended periods. Previous studies have shown that untreated or minimally processed organic waste materials may exhibit some degree of leaching or fragmentation. To mitigate this, various pre-treatment methods such as drying, chemical activation, or pyrolysis have been employed to enhance the mechanical stability and reusability of such materials. For example, treating cow dung biochar with phosphoric acid has been shown to enhance its porosity and adsorption efficiency, which in turn improves its structural stability in aqueous environments (Huating *et al*. 2024). Likewise, research has shown that chemical modification and thermal activation of cow dung ash significantly enhance its structural integrity and adsorption effectiveness (Ojeme *et al*. 2019). These findings suggest that appropriate treatment of cow dung-based adsorbents can address concerns related to their stability and potential leaching in water treatment applications.

This work's objective was to evaluate the effectiveness of acid-activated cow dung in eliminating artificial MG from watery solutions. This study aims to demonstrate cow dung's potential as an environmentally friendly and economical adsorbent for wastewater treatment by examining important variables like MG concentration, temperature, contact time, and pH. In the end, the results benefit public health and the environment by helping to design sustainable ways for handling wastewater contaminated with dyes.

## EXPERIMENTAL

### Materials

*Reagents*

All of the analytical-grade reagents used came from Sigma-Aldrich in India. For this investigation, methylene blue ($CH_{16}H_{18}N_3SCl.XH_2O$), molecular weight of 319.86 g/mol, and a λmax of 665 nm, was used. A 1000 ppm dye stock solution was created, and using serial dilution, solutions with different concentrations were generated from the stock solution.

*Preparation and characterization*

The animal waste was gathered at a cow market in Ibadan, Oyo State, Nigeria. The collected cow dung was sun-dried for seven days to get rid of the odor and stop maggot activity. The cow dung was then oven-dried at 80 °C for 3 h to eliminate any last traces of moisture. It was crushed into a powder with a mortar and pestle, sieved, and stored in a tightly sealed bottle before use. The cow manure was further activated by acid. The totally dried adsorbent was activated by Odoemelam *et al*. (2011) using the acid-activation and base-activation processes. A total of 50 g of the biosorbent was allowed to soak in a 1 M HCl solution for 12 h at 25 °C. After filtering the mixture, the material was dried on the bench, and to further remove the moisture, it was placed in an oven at 100 °C for 2 h.

The functional groups were measured in the range of 650 to 4000 $cm^{-1}$ with FT-IR (Fourier transform infrared spectroscopy; model 84005; Shimadzu, Japan) with an operational resolution of 2.0 $cm^{-1}$. The KBr approach was used. A scanning electron microscope was utilized to investigate the morphology of the cow dung (SEM, EVO-18, Zeiss, Germany). After being vacuum-dried, the samples were placed on double-sided tape, spray-coated with gold, and viewed at 5000x magnification.

## Batch Adsorption Studies

In this test, 100 mL of aqueous MB solution with varying weights of cow dung and a pH of 2 to 6 and a known concentration (50 to 300 mg/L) were utilized in six 250-mL Erlenmeyer flasks. Until an equilibrium condition was achieved, a water bath with a shaker was utilized. The appropriate amount of biosorbent was added to each flask, and samples were taken at specific times throughout the incubation period. Each sample's suspension was shaken, centrifuged at 4000 rpm, filtered, and MB concentration was measured at 650 nm wavelength using a UV-visible spectrophotometer (Jenway 7325 model, Jenway, Cole-Parmer Ltd., UK) at predetermined intervals to assess the MB dye's adsorption capacity.

The formula in Eqs. 1 and 2 below was used to determine the amount of MB sorbed at equilibrium and the percentage removal under equilibrium conditions,

$$\%DR = \frac{C_i - C_e}{C_i} \tag{1}$$

$$q_e = C_i - C_e \frac{V}{W} \tag{2}$$

where %DR is an acronym for percentage dye removal; $C_i$ and $C_e$ represent dye concentrations prior to and following biosorption in mg/L, respectively; W represents the sorbents' mass in g, and V represents the volume of MB in L; $q_e$ depicts MB amount sorbed at equilibrium in mg/g.

## Kinetics and Isotherms Evaluation

Table 1 below provides specifics regarding the kinetics models and isotherms utilized in this investigation:

**Table 1.** Kinetics Models and Isotherms

| Models | Equations | Parameters | References |
|---|---|---|---|
| Pseudo-first-order | $\log(q_e - q_t) = \log q_e - {k_1}/{2.303}t$ (3) | $q_t$ denotes adsorption capacity at time t (mg/g), t is time (min), while the rate constant is depicted as $k_1$ ($min^{-1}$) | Akpomie *et al.* (2019); Chauhan *et al.* (2023) |
| Pseudo-second- order | ${t}/{q_t} = {1}/{k_2} q_t + {t}/{q_e}$ (4) | $k_2$ stands for the second order rate constant (g/mg·min) | Chauhan *et al.* (2023) |
| Intraparticle Diffusion Model (IDM) | $Q_t = k_P t^{1/2} + C_i$ (5) | $k_p$ denotes rate constant for IDM (mg/g/$min^{1/2}$), and $C_i$ stands for the thickness of the boundary layer | El-Rayyes *et al.* (2025) |
| Langmuir | ${C_e}/{q_e} = {1}/{bq_m} + {C_e}/{q_m}$ (6) | Maximum adsorption capacity given as $Q_{max}$ (mg/g), and b is the Langmuir constant in L/mg | Ogundiran *et al.* (2022); El-Rayyes *et al.* (2025) |
| Separation factor ($R_L$) | $R_L = {1}/{(1+bC_o)}$ (7) | b as defined above | Ofudje *et al.* (2023) |
| Freundlich | $Inq_e = InK_F + {1}/{n} C_e$ (8) | $K_F$ (mg/g) is the constant of Freundlich and n is the adsorption intensity parameter | Ogundiran *et al.* (2022); El-Rayyes *et al.* (2025) |

The root mean square error is given as (Ho and McKay, 1999):

$$RMSE = \sqrt{\frac{\sum_i^N (Q_{(\exp)} - Q_{(cal)})^2}{N}} \qquad (9)$$

where N stands for data point.

## RESULTS AND DISCUSSION

### Cow Dung Characterization

Figure 1 depicts the main functional groups available in the treated cow dung (TDC) both before and after the uptake of MG. It was shown to include several functional groups that are essential for MB adsorption. The discovery of notable peaks at 3470 to 3655 $cm^{-1}$, 1765 $cm^{-1}$, and 1125 to 1095 $cm^{-1}$ that correlated with the -OH, $-NH_2$, C=O, and C-O groups suggests that cow dung may interact with dye molecules, particularly methylene blue (Ahmed *et al.* 2020; Chen *et al.* 2022). These groups are essential to MB's binding to the adsorbent, as evidenced by changes in the absorption bands with shifts in peak positions in the spectrum analysis that followed the adsorption process. At 3498 to 3662 $cm^{-1}$, 1770 $cm^{-1}$, and 1136 to 1090 $cm^{-1}$, new peaks were discovered that corresponded to the -OH, $-NH_2$, C=O, and C-O groups. The like $NH_2$, O-H, C=N, C-O, and Si-O-Si, including C=C groups, showed a little shift after adsorption indicating their role in the adsorption process (Ahmed *et al*. 2020).

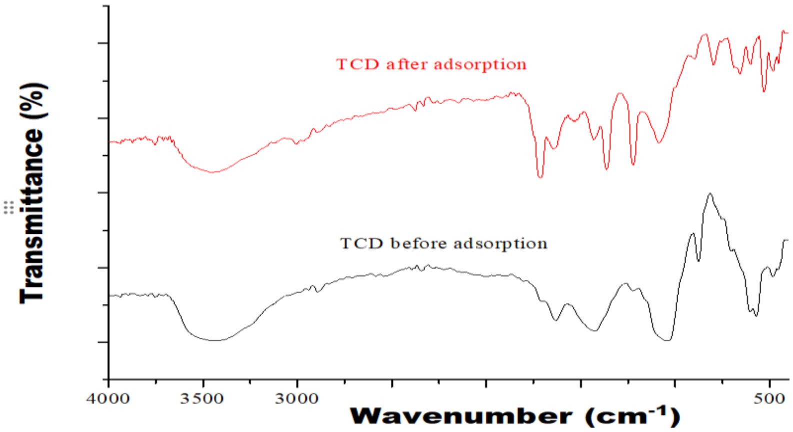


**Fig. 1.** FT-IR spectrum of cow dung before and after adsorption of methylene blue dye

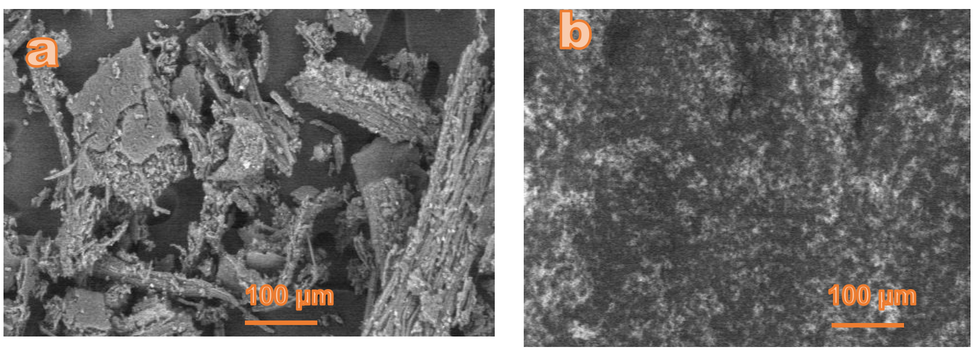


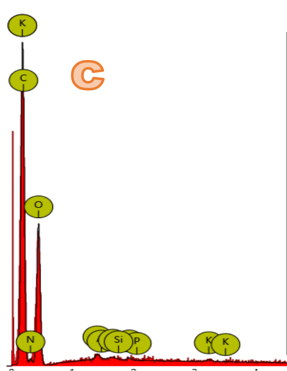


| Element Symbol | Atomic Conc. | Weight Conc. |
|---|---|---|
| C | 55.22 | 49.15 |
| O | 30.24 | 41.22 |
| Si | 10.61 | 6.75 |
| N | 3.5 | 2.11 |
| K | 0.27 | 0.33 |
| Al | 0.04 | 0.28 |
| P | 0.02 | 0.16 |

**Fig. 2.** SEM pictures that depict the appearance of TCD before (a), after (b) MB adsorption and (c) elemental composition of TCD.

A high surface area is indicated by the image's highly porous and fibrous structure for the TCD prior to adsorption (Fig. 2a). The uneven voids and rough roughness point to a high potential for adsorption. The surface of TCD becomes less rough and more uniform following adsorption, suggesting that the deposited MB molecules have probably covered the surface (Fig. 2b). The less obvious porosity character raises the possibility that the sites of adsorption were occupied. According to the general morphology, the surface has been covered by MB molecules, which has decreased the surface's roughness and accessible pores. The Energy Dispersive X-ray Spectroscopy (EDS) analysis of raw cow dung (Fig. 2c) reveals a composition dominated by organic elements, primarily carbon (C) and oxygen (O). Carbon constitutes 55.22% of the atomic concentration and 49.15% by weight, while oxygen accounts for 30.24% atomic and 41.22% weight. These high values indicate that raw cow dung is rich in organic matter, which is expected given its origin as a natural biological waste product. The presence of nitrogen (N) at 3.5% atomic concentration and 2.11% by weight further supports this, as nitrogen is a key component of proteins, urea, and other organic nitrogenous compounds commonly found in animal waste. Silicon (Si) is the most significant inorganic element identified, present at 10.61% atomic concentration and 6.75% by weight. This likely originates from the fibrous plant material in the cow's diet, such as grass. Trace elements such as potassium (K), aluminum (Al), and phosphorus (P) are also present in small amounts.

## Studies of Batch Experiments

At a pH of 5.0, RCD and TCD both showed optimal dye removal rates of 76.3% and 86.8%, respectively (Fig. 3). The ionization of the pigment molecules and the adsorbent's surface charge are responsible for this phenomena. The pH at which the surface of an adsorbent has a neutral charge is known as the point of zero charge (pHpzc), and it is a crucial adsorption characteristic. The pHpzc values for treated cow dung (TCD) and raw cow dung (RCD) are 4.53 and 4.16, respectively. This indicates that the adsorbent interface is positive at pH values lower than pHpzc, which causes electrostatic repulsion with cationic contaminants like MB (Ofudje *et al*. 2024; El-Rayyes *et al*. 2025). In contrast, the surface develops a negative charge for pH values higher than pHpzc, which improves adsorption by attracting MB molecules electrostatically. Because MB is a cationic dye, its adsorption works best when the substance being absorbed is negatively charged, which happens at pH > pHpzc. Because RCD's pHpzc is 4.16 and TCD's is 4.53, MB adsorption should work better at pH values higher than 5. Furthermore, TCD typically shows a greater potential for adsorption than RCD, most likely as a result of alterations that improve its functional groups, surface area, and porosity.

The cow dung surface and the MB cationic molecules interact electrostatically to drive the adsorption process. At higher pH values, positively charged particles in an aqueous MB dye solution facilitate adsorption onto negatively charged surfaces, whereas at lower pH values, the process is impeded (Ofudje *et al*. 2024). Oyebola *et al.* (2025) state that while the surface of the adsorbent is positive under low pH (acidic) conditions, resulting in electrostatic repulsion with the positively charged pollutant, more active sites on the surface of the untreated adsorbent become available as the pH rises from 2 to 5, improving its binding ability. This repulsion, however, lessens or even becomes attractive when the pH rises, allowing for more adsorption.

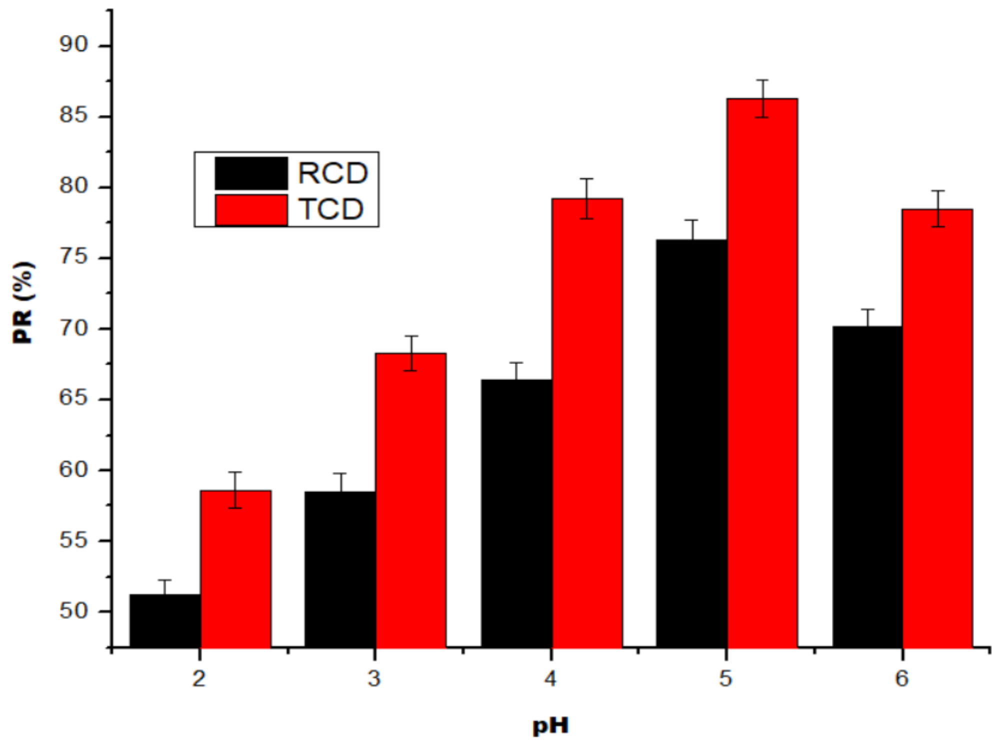


**Fig. 3.** pH role on the sorption of MB by RCD and TCD

Figures 4 and 5 show that the best time dye removal for RCD and TCD, respectively, was achieved after 120 and 100 min of contact. In the early stages, dye uptake increased sharply because of the availability of numerous sorption sites on the sorbent surface. However, as the system approached equilibrium, adsorption rates decreased, indicating that the sites that were accessible were saturated (Ahmed *et al*. 2020; El-Rayyes *et al*. 2025).

The amount of dye adsorbed increased as dye concentrations increased, declining at 300 mg/L, according to an evaluation of adsorption capacity in relation to MB concentration (Figs. 4 and 5). The amount sorbed surged from 19.5 mg/g to 58.5 mg/g for RCD in addition to 22.9 to 83.2 g for TCD as the concentration rose from 50 to 300 mg/L. According to the observed trend, more MB molecules can occupy available adsorption sites when the mass transfer driving power is increased by greater starting concentrations. There exists a relationship between MB concentration and the amount of MG sorbed because adsorption can flourish when the dye concentration increases as it removes all mass transfer barriers between the aqueous and solid phases (Ogundiran *et al.* 2022).

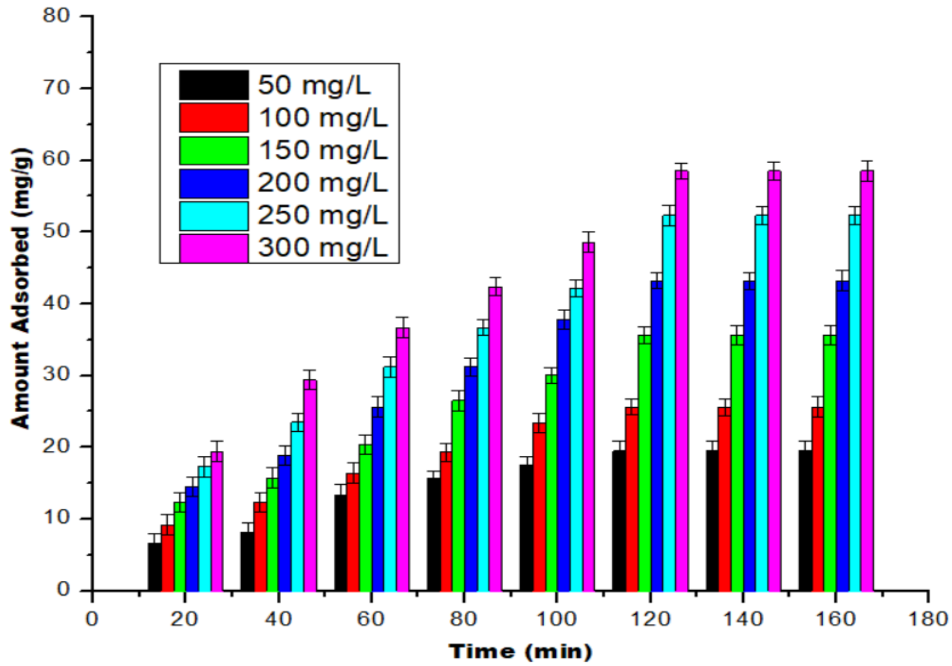


**Fig. 4.** Concentration of MB and contact time impacts on the sorption capacity of RCD

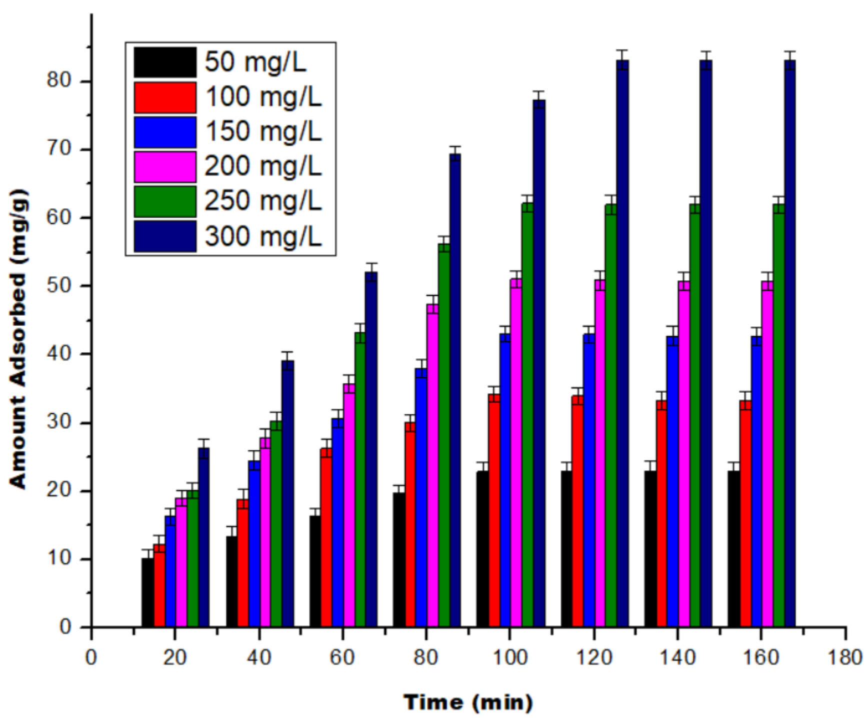


**Fig. 5.** Concentration of MB and contact time impacts on the sorption capacity of TCD

Figure 6 illustrates the percentage of elimination of MB as a function of sorbent dose. With an optimal removal effectiveness of 75.3% and 80.5% for RCD and TCD, respectively, at 0.5 g of adsorbent dosage, it was discovered that MB removal increased initially as cow dung dose increased. Once the dosage of 0.5 g was reached, however, the amount of MG removed from the solution did not increase, indicating that the adsorbent had reached its optimum level for dye adsorption. Similar to studies in the literature, this could be the result of the dye molecules accumulating or aggregating on the various adsorption sites, which would reduce the surface area and adsorption efficiency (Shukla *et al.* 2000; Ogundiran *et al*. 2022).

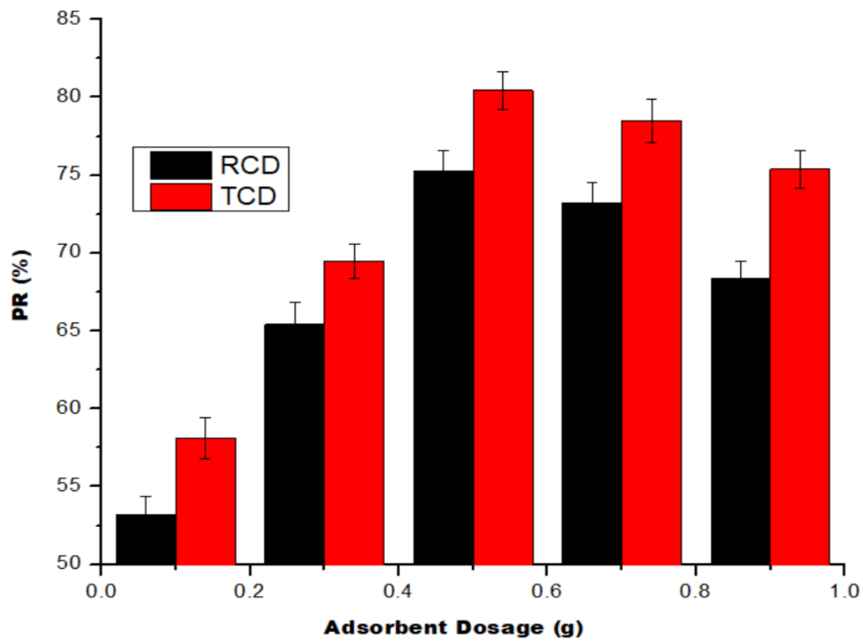


**Fig. 6.** Plot of adsorbent dosage on the removal of MB by RCD and TCD

Because the maximum rate of removal of 74.5% and 83.4% were observed at 50 °C for both RCD and TCD, respectively, Fig. 7 illustrates how temperature influences the efficacy of MB removal. According to this temperature relationship, the dye molecules' kinetic energy increases with temperature, making it simpler for them to interact with the acidified cow dung adsorbent. However, around 50 °C, the adsorption capacity decreased, most likely because the bindings between the dye and the adsorbent broke or the adsorbed molecules desorbated from the pores, which reduced the attractive forces between the two substances (Oyebola *et al.* 2025).

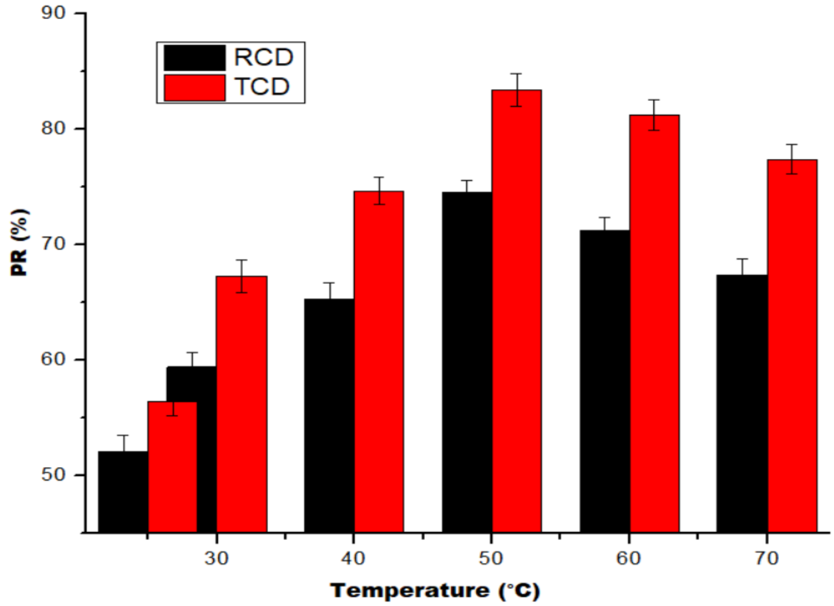


**Fig. 7.** Plots of removal efficiency against temperature by RCD and TCD

## Kinetics and Isotherms Studies

Kinetic modeling of the adsorption data was done using pseudo-first-order, pseudo-second-order, and intraparticle diffusion kinetics models, the plots of which are displayed in Figs. 8 to 10. The parameters for these fits are listed in Tables 1 and 2. The RCD shows a reasonably excellent model fit in terms of first-order kinetics ($R^2$ values are typically above 0.9), and the predicted $Q_e$ values are consistently near the experimental findings. The first-order rate constant ($k_1$) for TCD, on the other hand, is lower (varying from 0.019 to 0.028 min$^{-1}$), and although the model fit is respectable ($R^2$ = 0.96 to 0.99), the larger percentage SSE values show that this model does not reflect adsorption in TCD. However, with $R^2$ values near 0.997, the second-order kinetic model offers a far better fit for TCD, across all MB concentrations. The RCD, on the other hand, has more variable $R^2$ values (ranging from 0.587 to 0.985). Furthermore, TCD consistently has a higher second-order rate constant ($k_2$), indicating that this model is dominating. This model's reduced TCD percentage SSE values further support its applicability in explaining the adsorption process.

Additionally, the intraparticle diffusion model fits both RCD and TCD well ($R^2 >$ 0.99), suggesting that pore diffusion is important for MB adsorption. Faster diffusion in TCD is indicated by the notably larger intraparticle diffusion rate constant ($K_p$) for TCD, particularly at higher MB concentrations. Furthermore, TCD regularly has bigger intercept (Ci) values, indicating a stronger boundary layer impact and the significant role of surface adsorption. At all MB concentrations, TCD shows a substantially greater adsorption capacity than RCD. The second-order kinetic model best describes the adsorption process for TCD, but the first-order model worked better for RCD. The enhanced boundary layer effect in TCD implies that surface adsorption is also a crucial component, even if intraparticle diffusion is a significant mechanism for both adsorbents.

While the pseudo-second-order model provided the best statistical fit for TCD, this does not necessarily imply a chemisorption mechanism in isolation, however, with the information gathered from the intraparticle diffusion model, there is a likelihood that the overall adsorption process is diffusion-controlled, particularly into a network of fine pores; a mechanism consistent with the structure of biomass-based adsorbents like sorghum husks ( Hubbe *et al.*, 2019).

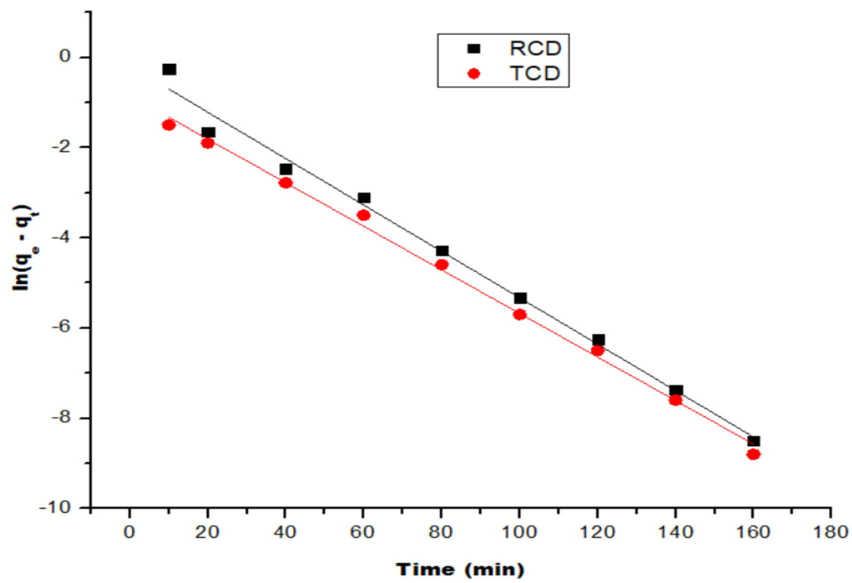


**Fig. 8.** Pseudo-first-order plot for the adsorption of MB by RCD and TCD

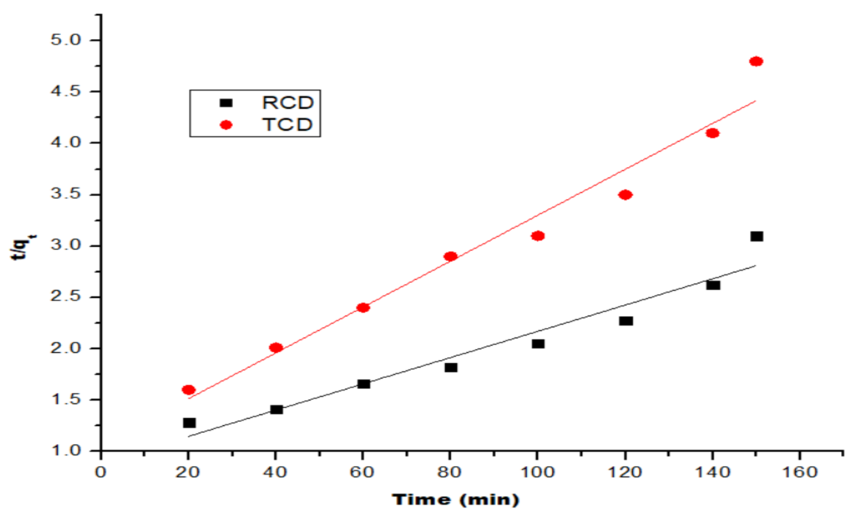


**Fig. 9.** Pseudo-second-order plot for the adsorption of MB by RCD and TCD

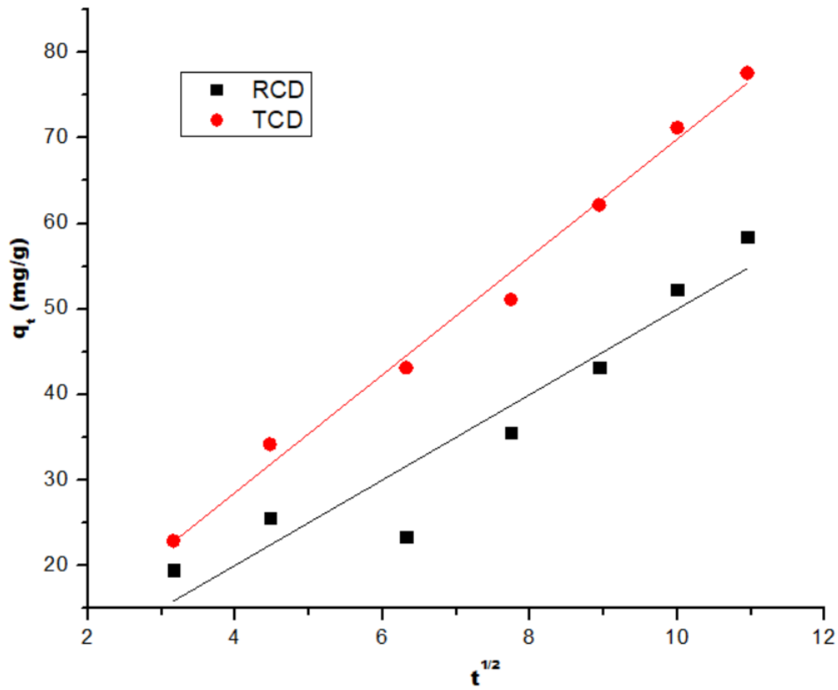


**Fig. 10.** Intraparticle diffusion model plot for the adsorption of MB by RCD and TCD

**Table 1.** Kinetics Constants for the Sorption of MB by RCD

| | | First Order | | | | Second Order | | | | Intra Particle Diffusion | | |
|---|---|---|---|---|---|---|---|---|---|---|---|---|
| **$C_o$** (mg/L) | **$Q_{e(exp)}$** (mg $g^{-1}$) | $Q_{e\ cal}$ (mg $g^{-1}$) | $k_1$ ($min^{-1}$) | **$R^2$** | **% SSE** | $Q_{e\ cal}$ (mg $g^{-1}$) | $k_2$ (g $mg^{-1}$ $min^{-1}$) | **$R^2$** | **% SSE** | $Kp$ (mg $g^{-1}$ $min^{-0.5}$) | $C_1$ (mg $g^{-1}$) | **$R^2$** |
| 50 | 19.5 | 20.12 | 0.115 | 0.987 | 0.010 | 24.31 | 0.062 | 0.587 | 0.074 | 1.819 | 0.175 | 0.991 |
| 100 | 23.500 | 21.34 | 0.135 | 0.924 | 0.028 | 37.26 | 0.027 | 0.985 | 0.177 | 3.934 | 0.398 | 0.994 |
| 150 | 36.400 | 38.22 | 0.183 | 0.992 | 0.015 | 42.35 | 0.331 | 0.967 | 0.049 | 6.189 | 0.860 | 0.989 |
| 200 | 43.200 | 45.79 | 0.225 | 0.912 | 0.018 | 51.22 | 0.338 | 0.674 | 0.056 | 7.096 | 1.222 | 0.994 |
| 250 | 52.100 | 54.65 | 0.271 | 0.943 | 0.015 | 60.98 | 0.447 | 0.884 | 0.051 | 8.931 | 1.552 | 0.995 |
| 300 | 68.500 | 67.02 | 0.298 | 0.078 | 0.007 | 75.600 | 0.632 | 0.854 | 0.031 | 11.091 | 1.704 | 0.993 |

**Table 2.** Kinetics Constants for the Sorption of MB by TCD

| | | First Order | | | | Second Order | | | | Intra Particle Diffusion | | |
|---|---|---|---|---|---|---|---|---|---|---|---|---|
| **$C_o$** (mg/L) | **$Q_{e(exp)}$** (mg $g^{-1}$) | $Q_{e\ cal}$ (mg $g^{-1}$) | $k_1$ ($min^{-1}$) | **$R^2$** | **% SSE** | $Q_{e\ cal}$ (mg $g^{-1}$) | $k_2$ (g $mg^{-1}$ $min^{-1}$) | **$R^2$** | **% SSE** | $Kp$ (mg $g^{-1}$ $min^{-0.5}$) | $C_1$ (mg $g^{-1}$) | **$R^2$** |
| 50 | 22.980 | 33.21 | 0.028 | 0.978 | 0.134 | 23.434 | 0.017 | 0.997 | 0.006 | 1.636 | 1.775 | 2.022 |
| 100 | 34.120 | 46.094 | 0.020 | 0.966 | 0.106 | 48.003 | 0.0634 | 0.996 | 0.123 | 1.784 | 3.522 | 2.176 |
| 150 | 42.330 | 55.565 | 0.023 | 0.984 | 0.094 | 43.924 | 0.262 | 0.993 | 0.011 | 3.442 | 5.871 | 4.674 |
| 200 | 50.600 | 64.759 | 0.027 | 0.978 | 0.084 | 51.258 | 0.056 | 0.997 | 0.004 | 5.861 | 7.249 | 9.295 |
| 250 | 62.300 | 72.596 | 0.022 | 0.996 | 0.050 | 61.304 | 0.160 | 0.970 | 0.005 | 5.765 | 9.356 | 8.478 |
| 300 | 83.200 | 89.983 | 0.019 | 0.991 | 0.025 | 82.593 | 0.286 | 0.995 | 0.002 | 5.813 | 12.430 | 6.595 |

The data plots for the isotherm are presented in Figs. 11 and 12, and Table 3 describes the computed parameters. The TCD has a greater maximum adsorption capacity (Qmax) than RCD (47.8 mg/g) in the Langmuir isotherm analysis, which is based on the assumption of a homogeneous surface. According to Oyebola *et al*. (2025), this implies that treatment increases adsorption capacity, most likely by improving surface characteristics or expanding the number of accessible binding sites. After treatment, MB adsorption is more effective because the separation factor ($R_L$) for TCD (0.26) is lower than that of RCD (0.72). The lower value for TCD indicates a stronger adsorption affinity because 0 < RL < 1 indicates favorable adsorption (Ogundiran *et al.* 2022). The Langmuir model's correlation coefficient ($R^2$) is greater for RCD (0.978) than for TCD (0.885), indicating that MB adsorption onto RCD more closely resembles the Langmuir model.

Important information is also provided by the Freundlich isotherm, which characterizes adsorption on a heterogeneous surface. Further demonstrating the enhanced adsorption effectiveness of treated cow dung, the Freundlich constant ($K_F$), which measures adsorption capacity, is higher for TCD (36.82 mg/g)(mg/L)$^{-1/2)}$ than for RCD (29.04 mg/g)(mg/L)$^{-1/2}$). The TCD has a higher adsorption affinity and more variety in binding sites, as indicated by the lower value of 1/n, which represents adsorption intensity, compared to RCD (0.470). Increased pores from the therapy procedure could be the cause of this. Furthermore, MB adsorption onto TCD more closely resembles the Freundlich model, as indicated by the correlation coefficient for the Freundlich model being greater for TCD (0.998) than for RCD (0.635). This implies that whereas RCD adheres to a more homogeneous adsorption pattern as defined by the Langmuir model, adsorption onto TCD takes place on a heterogeneous surface. The results of earlier research by Ogundiran *et al*. (2022) and Oyebola *et al*. (2025) corroborate the findings.

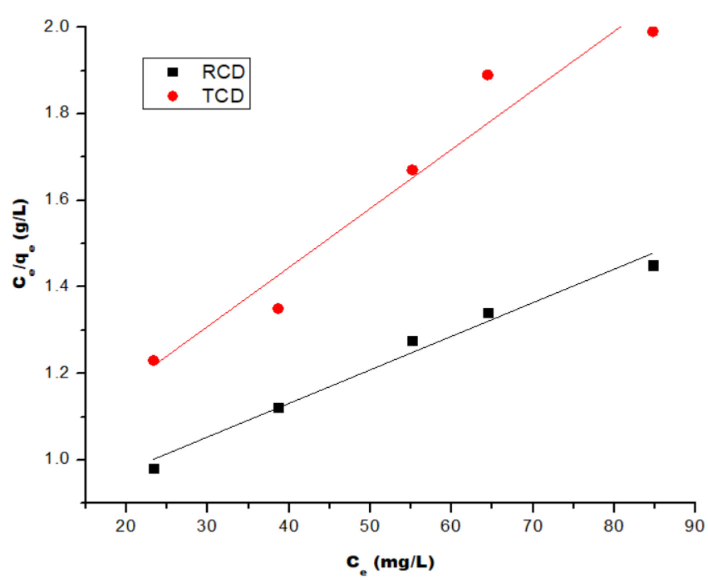


**Fig. 11.** Langmuir isotherm model for the uptake of MB by RCD and TCD

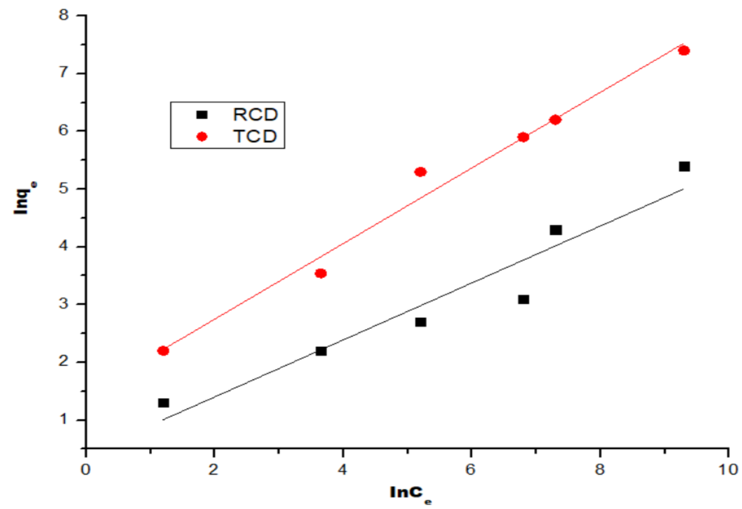


**Fig. 12.** Freundlich isotherm model for the uptake of MB by RCD and TCD

**Table 3.** Isotherm Constant for MB Sorption Using RCD and TCD

| | Parameters | RCD | TCD |
|---|---|---|---|
| **Langmuir** | $Q_{max}$ (mg/g) | 47.8 | 64.25 |
| | $R_L$ | 0.72 | 0.26 |
| | $R^2$ | 0.978 | 0.885 |
| **Freundlich** | $K_F$ (mg/g)(mg/L)$^{-1/2}$ | 29.04 | 36.82 |
| | 1/*n* | 0.740 | 0.470 |
| | $R^2$ | 0.635 | 0.998 |

With adsorption capabilities that are competitive with those of other materials described in the literature, raw and processed cow dung show great promise as inexpensive, environmentally acceptable adsorbents (Table 4). Because TCD outperforms a number of carbon- and bio-based materials, it is a good substitute for wastewater treatment applications.

**Table 4.** Adsorption Capacity Analysis of RCD and TCD in Relation to Related Literature Adsorbents

| Adsorbent | Adsorption Capacity (mg/g) | References |
|---|---|---|
| Modified biochar material | 5.018 | Hoslett *et al.* (2020) |
| Multi-walled carbon nanotubes filled with $Fe_2O3$ parti | 42.3 | Qu *et al.* (2008) |
| N-maleyl chitosan/P(AA-co-VPA) | 50.180 | Nakhjiri *et al.* (2018) |
| *Gigantochloa* Bamboo-Derived Biochar | 86.60 | Suhaimi et al. (2022) |
| Coconut husk based activated carbon | 66 | Tamai *et al.* (1996) |
| Lignin and chitosan | 36 | Albadarin *et al.* (2017) |
| Fly ash | 50.27 | Wang *et al.* (2023) |
| Algerian goethite | 7.09 | Manal *et al.* (2024) |
| Untreated sugarcane biomass | 24.457 | Ofudje *et al.* (2024) |
| Treated sugarcane biomass | 32.315 | Ofudje *et al.* (2024) |
| Raw cow dung | 47.8 | This work |
| Treated cow dung | 64.25 | This work |

## Thermodynamic Studies

Entropy change (ΔS°), Gibbs free energy (ΔG°), and changing the enthalpy (ΔH°) are examples of thermodynamic characteristics that support the adsorption nature and are useful in determining the spontaneity and feasibility of the adsorption nature (Fig. 13). These thermodynamic constants were estimated from the expression below (Ademoyegun *et al.* 2022; El-Rayyes *et al.* 2025),

$$K_d = {q_e}/{C_e} \tag{10}$$

$$\ln K_d = {\Delta S^o}/{R} - {\Delta H^o}/{RT} \tag{11}$$

$$\Delta G^o = RTInK_d \tag{12}$$

where temperature in K is denoted as T and the universal gas constant in 8.304 J $mol^{-1}K^{-1}$ is given as R. The values in Table 5 and ΔG° (Kadirvelu 2013) were determined using Eq. 11. The MB adsorption onto both RCD and TCD is spontaneous, as indicated by the negative values of ΔG° at all temperatures. Additionally, ΔG becomes increasingly negative as temperature rises, indicating that higher temperatures improve adsorption efficiency (Macedo 2016; Ofudje *et al*. 2024). At all temperatures, however, TCD shows fewer negative ΔG values than RCD, suggesting that MB adsorption onto TCD is marginally less spontaneous than onto RCD. This explains why, when the system absorbs heat to promote MB binding, adsorption efficiency increases with temperature. Because of changes in surface chemistry that increase adsorption efficiency following treatment, TCD's lower ΔH value indicates that the adsorption process uses less energy than RCD. A rise in randomness at the solid-liquid interface during adsorption is shown by the positive entropy change values for both RCD (4.32 J/mol.K) and TCD (1.42 J/mol.K) (Ademoyegun *et al.* 2022; Oyebola *et al.* 2025). This implies that when MB molecules move from the solution phase to the adsorbent surface, they become more disorganized.

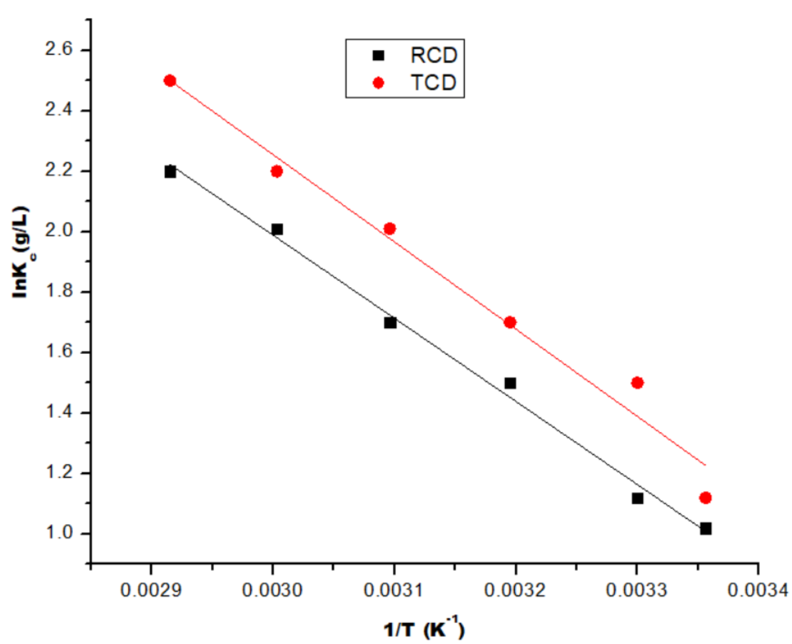


**Fig. 13**. Plot of thermodynamics for the sorption of MB by RCD and TCD

**Table 5.** Thermodynamic Variables for the Sorption of Methylene Blue Dye onto RCD and TCD

| | RCD | | | TCD | | |
|---|---|---|---|---|---|---|
| T (°C) | ΔG (kJ/mol) | ΔH (kJ/mol) | ΔS (kJ/mol) | ΔG (kJ/mol) | ΔH (kJ/mol) | ΔS (kJ/mol) |
| 25 | -1.25 | | | -0.89 | | |
| 30 | -2.33 | | | -1.43 | | |
| 40 | -4.46 | 9.32 | 4.32 | -2.27 | 6.4 | 1.42 |
| 50 | -5.56 | | | -3.3 | | |
| 60 | -6.25 | | | -3.8 | | |
| 70 | -6.83 | | | -4.6 | | |

## CONCLUSIONS

1. Both raw and activated cow dung were used to remove methylene blue (MB) dye from solutions.
2. The presence of key functional groups such as –OH, $–NH_2$, C=O, and C–O in cow dung highlights its potential for effective interaction with methylene blue molecules.
3. Following MB adsorption, the SEM examination clearly shows a change in TCD's surface structure, including a smoother surface and a decrease in porosity, proving TCD's promise as an efficient and reasonably priced adsorbent.
4. After adjusting the conditions, more than 80% of the dye was adsorbed, demonstrating that acid activated cow dung was an economical and effective sorbent for dye removal.
5. The Freundlich model fits TCD better and reflects the effect of treatment on increasing adsorption efficiency, whereas the Langmuir model better captures adsorption onto RCD.
6. All things taken into account, the thermodynamic study verifies that MB adsorption onto RCD and TCD is an endothermic, spontaneous process that becomes more effective at increasing temperatures.

## ACKNOWLEDGMENTS

The authors extend their appreciation to the financial support *via* the the Ongoing Research Funding program, (ORF-2025-754), King Saud University, Riyadh, Saudi Arabia, for funding this research.

## REFERENCES CITED

Ademoyegun, A. J., Babarinde, N. A. A., and Ofudje, E. A. (2022). "Sorption of Pb(II), Cd(II), and Zn(II) ions from aqueous solution using *Thaumatococcus danielli* leaves:

Kinetic, isotherm, and thermodynamic studies," *Desalination & Water Treatment* 273, 162-171. DOI: 10.5004/dwt.2022.28877

Ahmad, A., Khan, N., Giri, B. S., Chowdhary, P., and Chaturvedi, P. (2020). "Removal of methylene blue dye using rice husk, cow dung and sludge biochar: Characterization, application, and kinetic studies," *Bioresource Technology* 306, Article ID 123202. DOI: 10.1016/j.biortech.2020.123202

Ahmad, A., Mohd-Setapar, S. H., Chuong, C. S., Khatoon, A., Wani, W. A., Kumar, R., and Rafatullah, M. (2015). "Recent advances in new generation dye removal technologies: Novel search for approaches to reprocess wastewater," *RSC Advances* 5(81), 30801-30818. DOI: 10.1039/C4RA16959J

Akpomie, K. G., Fayomi, O. M., Ezeofor, C. C., Sha'Ato, R., and Van Zyl, W. E. (2019). "Insights into the use of metal complexes of thiourea derivatives as highly efficient adsorbents for ciprofloxacin from contaminated water," *Transactions of the Royal Society of South Africa* 74(2), 180-188. DOI: 10.1080/0035919x.2019.1614695

Albadarin, A. B., Collins, M. N., Naushad, M., Shirazian, S., Walker, G., and Mangwandi, C. (2017). "Activated lignin-chitosan extruded blends for efficient adsorption of methylene blue," *Chemical Engineering Journal* 307, 264–272. DOI: 10.1016/j. cej.2016.08.089

Bielska, M., and Szymanowski, J. (2006). "Removal of methylene blue from waste water using micellar enhanced ultrafiltration," *Water Research* 40(5), 1027-1033. DOI: 10.1016/j.watres.2005.12.027

Chauhan, S., Shafi, T., Dubey, B. K., and Chowdhury, S. (2023). "Biochar-mediated removal of pharmaceutical compounds from aqueous matrices *via* adsorption," *Waste Disposal Sustainable Energy* 5, 37–62. DOI: 10.1007/s42768-022-00118-y

Chen, X., Yu, G., Chen, Y., Tang, S., and Su, Y. (2022). "Cow dung-based biochar materials prepared *via* mixed base and its application in the removal of organic pollutants," *International Journal of Molecular Sciences* 23(17), Article Number 10094. DOI: 10.3390/ijms231710094

Crini, G., and Lichtfouse, E. (2019). "Advantages and disadvantages of techniques used for wastewater treatment," *Environmental Chemistry Letters* 17(1), 145-155. DOI: 10.1007/s10311-018-0785-9

Dawood, S., Gupta, T., and Sen, T. (2017). "Adsorptive removal of methylene blue (MB) dye at kaolin clay-water interface: Kinetics, isotherm modelling and process design. In: *Clay Minerals: Properties, Occurrence and Uses*, Nova Science, New York, NY, USA, pp. 209-236.

El-Rayyes, A., Arogundade, I., Ogundiran , A. A., Hefnawy, M., Ofudje, E. A., El Gamal, A., Lamia, A. A., and Alsuhaibani, A. M. (2025). "Hot water-treated cow waste use as an efficient adsorbent for cresol red dye and chromium VI removal from aqueous solutions," *BioResources* 20(2), 3252–3285. DOI: 10.15376/biores.20.2.3252-3285

Faraji, H., Mohamadi, A. A., Soheil Arezomand, H. R., and Mahvi, A. H. (2015). "Kinetics and equilibrium studies of the removal of blue basic 41 and methylene blue from aqueous solution using rice stems," *Iranian Journal of Chemistry and Chemical Engineering (IJCCE)* 34(3), 33-42.

Geed, S. R., Samal, K., and Tagade, A. (2019). "Development of adsorption-biodegradation hybrid process for removal of methylene blue from wastewater," *Journal of Environmental Chemical Engineering* 7(6), Article ID 103439.DOI: 10.1016/j.jece.2019.103439

Ho, Y. S., and McKay, G. (1999). "Pseudo-second order model for sorption processes," *Process Biochemistry* 34(5), 451–465. DOI: 10.1016/S0032-9592(98)00112-5

Hoslett, J., Ghazal, H., Mohamad, N., and Jouhara, H. (2020). "Removal of methylene blue from aqueous solutions by biochar prepared from the pyrolysis of mixed municipal discarded material," *Science of The Total Environment* 714, Article ID 136832. DOI: 10.1016/j.scitotenv.2020.136832

Huating, J., Xiang, L., and Yingjie, D. (2024). "Phosphoric acid activation of cow dung biochar for adsorbing enrofloxacin in water: Icing on the cake," *Environ Pollut*. 341, 122887. DOI 10.1016/j.envpol.2023.122887.

Hubbe, M. A., Azizian, S., and Douven, S. (2019). "Implications of apparent pseudo-second-order adsorption kinetics onto cellulosic materials. A review," BioResources 14(3), 7582-7626. DOI: 10.15376/biores.14.3.7582-7626.

Iwuozor, K. O., Emenike, E. C., Aniagor, C. O., Iwuchukwu, F. U., Ibitogbe, E. M., Temitayo, O. B., Omuku, P. E., and Adeniyi, A. G. (2022). "Removal of pollutants from aqueous media using cow dung-based adsorbents," *Current Research in Green and Sustainable Chemistry* 5, Article ID 100300. DOI: 10.1016/j.crgsc.2022.100300

Manal, L., Mohammed, R. R., Mohammed, M. S., Aissaoui, Z., and Lazhar, H. (2024). "Experimental study of methylene blue adsorption from aqueous solutions onto natural Algerian goethite," *Water Practice & Technology* 19(8), Article Number 3297 DOI: 10.2166/wpt.2024.191

Mashkoor, F., and Nasar, A. (2020). "Magsorbents: Potential candidates in wastewater treatment technology–A review on the removal of methylene blue dye," *Journal of Magnetism and Magnetic Materials* 500, Article ID 166408. DOI: 10.1016/j.jmmm.2020.166408

Métivier-Pignon, H., Faur-Brasquet, C., and Le Cloirec, P. (2003). "Adsorption of dyes onto activated carbon cloths: Approach of adsorption mechanisms and coupling of ACC with ultrafiltration to treat coloured wastewaters," *Separation and Purification Technology* 31(1), 3-11. DOI: 10.1016/S1383-5866(02)00147-8

Nakhjiri, M. T., Marandi, G. B., and Kurdtabar, M. (2018). "Poly (AA-co-VPA) hydrogel cross-linked with N-maleyl chitosan as dye adsorbent: Isotherms, kinetics and thermodynamic investigation," *International Journal of Biological Macromolecules* 117, 152-166. DOI: 10.1016/j.ijbiomac.2018.05.140

Ofudje, E. A., Al-Ahmary, K. M., Alzahrani, E. A., Ud Din, S., and Al-Otaibi, J. S. (2024). "Sugarcane peel ash as a sorbent for methylene blue," *BioResources* 19(4), 9191-9219. DOI: 10.15376/biores.19.4.9191-9219

Ofudje, E. A., Sodiya, E. F., Olanrele, O. S., and Akinwunmi, F. (2023). "Adsorption of $Cd^{2+}$ onto apatite surface: Equilibrium, kinetics and thermodynamic studies," *Heliyon* 9, Article Number e12971. DOI: 10.1016/j.heliyon.2023.e12971

Ogundiran, A. A., Ofudje, E. A., Ogundiran, O. O., and Adewusi, A. M. (2022). "Cationic dye adsorptions by eggshell waste: Kinetics, isotherms and thermodynamics studies," *Desalination & Water Treatment* 280, 157-167. DOI: 10.5004/dwt.2022.29080

Ojeme, V. C.; Ayodele, O.; Oluwasina, O. O.; and Okoronkwo, E. A. (2019). "Adsorption of Pb(II) ions from aqueous solutions using chemically treated and untreated cow dung ash," *BioRes*ources 14(2), 2622-2641. DOI: 10.15376/biores.14.2.2622-2641

Oveisi, M., Asli, M. A., and Mahmoodi, N. M. (2018). "MIL-Ti metal-organic frameworks (MOFs) nanomaterials as superior adsorbents: Synthesis and ultrasoundaided dye adsorption from multicomponent wastewater systems," *Journal of Hazardous Materials* 347, 123-140. DOI: 10.1016/j.jhazmat.2017.12.057

Oyebola, E. O., Hefnawy, M., Ofudje, E. A., El Gamal, A., Akande, J. A., and Emran, T. B. (2025). "Nickel ions biosorption onto sawmill wood waste products: Kinetics, equilibrium, and thermodynamic investigations," *BioResources* 20(2), 3024–3046. DOI: 10.15376/biores.20.2.3024-3046

Qian, Q., Chen, Q., Machida, M., Tatsumoto, H., Mochidzuki, K., and Sakoda, A. (2009). "Removal of organic contaminants from aqueous solution by cattle manure compost (CMC) derived activated carbons" *Applied Surface Science* 255(12), 6107-6114. DOI: 10.1016/j.apsusc.2009.01.060

Qian, Q., Machida, M., and Tatsumoto, H. (2008). "Textural and surface chemical characteristics of activated carbons prepared from cattle manure compost," *Waste Management* 28(6), 1064-1071. DOI: 10.1016/j.wasman.2007.03.029

Qu, S., Huang,F., Yu, S., Chen, G., and Kong, J. (2008). "Magnetic removal of dyes from aqueous solution using multi-walled carbon nanotubes filled with $Fe_2O_3$ particles," *Journal of Hazardous Materials* 160, 643–647. DOI: 10.1016/j.jhazmat.2008.03.037

Rafatullah, M., Sulaiman, O., Hashim, R., and Ahmad, A. (2010). "Adsorption of methylene blue on low-cost adsorbents: A review" *Journal of Hazardous Materials* 177(1-3), 70-80. DOI: 10.1016/j.jhazmat.2009.12.047

Santoso, E., Ediati, R., Kusumawati, Y., Bahruji, H., Sulistiono, D., and Prasetyoko, D. (2020). "Review on recent advances of carbon based adsorbent for methylene blue removal from waste water," *Materials Today Chemistry* 16, Article ID 100233. DOI: 10.1016/j.mtchem.2019.100233

Shahryari, Z., Goharrizi, A. S., and Azadi, M. (2010). "Experimental study of methylene blue adsorption from aqueous solutions onto carbon nano tubes," *International Journal of Water Resources and Environmental Engineering* 2(2), 016-028.

Shokoohi, R., Vatanpoor, V., Zarrabi, M., and Vatani, A. (2010). "Adsorption of Acid Red 18 (AR18) by activated carbon from poplar wood-A kinetic and equilibrium study," *Journal of Chemistry* 7(1), 65-72. DOI: 10.1155/2010/958073

Shukla, A., Dorris, K. L., and Zhang, Y. (2000). "The removal of heavy metal from aqueous solutions by sawdust adsorption-removal of copper," *Journal of Hazardous Materials* 80(1-3), 33-42. DOI: 10.1016/S0304-3894(00)00278-8

Sonwani, R. K., Swain, G., Giri, B. S., Singh, R. S., and Rai, B. N. (2020). "Biodegradation of Congo red dye in a moving bed biofilm reactor: Performance evaluation and kinetic modeling," *Bioresource Technology* 302, Article ID 122811. DOI: 10.1016/j.biortech.2020.122811

Suhaimi, N., Kooh, M. R. R., Chao, C.-T. C., Chau, Y.-F. C., Chiang, H.-P., Lim, C. M., Mahadi, A. H., Hassan, N. H. H., and Thotagamuge, R. (2022). "The use of *Gigantochloa* bamboo-derived biochar for the removal of methylene blue from aqueous solution," *Adsorption Science & Technology*, Article ID 8245797. DOI: 10.1155/2022/8245797

Tamai, H., Kakii, T., Hirota, Y., Kumamoto, T., and Yasuda, H. (1996). "Synthesis of extremely large mesoporous activated carbon and its unique adsorption for giant molecules," *Chem. Mater.* 8, 454–462. DOI: 10.1021/cm950381t

Tsai, W.-T., Huang, P.-C., and Lin, Y.-Q. (2019). "Reusing cow manure for the production of activated carbon using potassium hydroxide (KOH) activation process and its liquid-phase adsorption performance," *Processes* 7(10), Article Number 737. DOI: 10.3390/pr7100737

Wang, J., Tan, Y., Yang, H., Zhan, L., Sun, G., and Luo, L. (2023). "On the adsorption characteristics and mechanism of methylene blue by ball mill modified biochar," *Science Reports* 13, Article ID 21174. DOI: 10.1038/s41598-023-48373-1
Yang, Y., Zhu, Q., Peng, X., Sun, J., Li, C., Zhang, X., Zhang, H., Chen, J., Zhou, X., and Zeng, H. (2022). "Hydrogels for the removal of the methylene blue dye from wastewater: A review," *Environmental Chemistry Letters* 20(4), 2665-2685. DOI: 10.1007/s10311-022-01414-z
Yao, X., Ji, L., Guo, J., Ge, S., Lu, W., Cai, L., Wang, Y., Song, W., and Zhang, H. (2020). "Magnetic activated biochar nanocomposites derived from wakame and its application in methylene blue adsorption," *Bioresource Technology* 302, Article ID 122842 DOI: 10.1016/j.biortech.2020.122842
Zhu, Y., Yi, B., Hu, H., Zong, Z., Chen, M., and Yuan, Q. (2020). "The relationship of structure and organic matter adsorption characteristics by magnetic cattle manure biochar prepared at different pyrolysis temperatures," *Journal of Environmental Chemical Engineering* 8(5), Article ID 104112. DOI: 10.1016/j.jece.2020.104112
Zhu, Y., Yi, B., Yuan, Q., Wu, Y., Wang, M., and Yan, S. (2018). "Removal of methylene blue from aqueous solution by cattle manure-derived low temperature biochar," *RSC Advances* 8(36), 19917-19929. DOI: 10.1039/C8RA03018A

Article submitted: April 3, 2025; Peer review completed: May 18, 2025; Revisions accepted: June 22, 2025; Published: June 25, 2025.
DOI: 10.15376/biores.20.3.6815-6836